A REGULARIZED MESH TRANSFORMATION METHOD FOR THE COMPUTATION OF CRYSTALLINE MICROSTRUCTURES

ZHIPING LI

LMAM & SCHOOL OF MATHEMATICAL SCIENCES,
PEKING UNIVERSITY, BEIJING 100871, P.R.CHINA

ABSTRACT. Since the finite element approximations of microstructures are strongly mesh dependent, the use of the mesh transformation method based on the energy minimizing principle is considered a natural approach in the finite element computation of microstructures. However, without a control on the mesh quality, the mesh can become increasingly irregular in the process of energy minimization and thus jeopardize the convergence of the algorithm. In this paper, a mesh quality control term based on the mesh regularity is introduced to regularize the mesh transformation procedure. The existence and convergence of the regularized mesh transformation method are proved. Numerical experiments show that the method does help to produce much better numerical results in the computation of microstructures.

1. INTRODUCTION

In the well known geometrically nonlinear theory of crystalline microstructure of Ball and James [1, 2], the static problem of austenitic-martensitic phase transitions is characterized by the problem of minimizing the elastic energy

$$F(u;\ \Omega) = \int_\Omega f(\nabla u(x),\ \theta(x))\, dx \tag{1.1}$$

in a set of admissible deformations

$$\mathbb{U}(u_0;\ \Omega) = \{u \in W^{1,p}(\Omega; \mathbb{R}^m) : u = u_0,\ \text{on } \partial\Omega_0\}, \tag{1.2}$$

1991 *Mathematics Subject Classification.* 73C50,65K10,65N30,49J45,49M20.

Key words and phrases. Nonconvex energy minimization, microstructure, regularized mesh transformation, mesh quality control.

The research was supported in part by the Special Funds for Major State Basic Research Projects (G1999032804), NSFC major project and RFDP of China.

where the Ericksen-James elastic energy density $f(\cdot,\ \theta)$ is such that $f(\cdot,\ \theta)$ has a unique potential well (austenite) above the transformation temperature ($\theta > \theta_T$) and has several symmetry related potential wells (martensite) below the transformation temperature ($\theta < \theta_T$) [1, 2, 3, 4], and where $\Omega \subset \mathbb{R}^n$, $n = 2$ or 3, is a bounded open set with a Lipschitz continuous boundary $\partial\Omega$, $\partial\Omega_0$ is a subset of $\partial\Omega$, θ is a given temperature field and $1 < p < \infty$.

Below the transformation temperature, for properly given boundary data u_0, the minimizing sequences of the elastic energy $F(\cdot;\ \Omega)$ in $\mathbb{U}(u_0;\ \Omega)$ will be essentially consist of finely laminated twins which are in the martensitic potential wells [1, 2]. Many numerical methods have been developed to compute the laminated microstructure (see [5] for a survey on the conforming and nonconforming finite element approximations, see also [6, 7, 8, 9, 10, 11, 12] among many others for more recent developments).

One of the main difficulties in finite element approximations of crystalline microstructures is that the numerical solution is strongly mesh dependent and, unless the mesh is properly provided, it often produces false information on the microstructure in question [5, 13, 14, 15, 16]. To avoid the mesh dependent of the finite element approximation, it is natural to involve the mesh distribution into the minimization procedure. The idea of the mesh transformation method (MTM), which is to minimize the elastic energy on all admissible finite element function spaces obtained by mesh distribution transformation, leads to the following discrete problem

$$(MTM) \quad \begin{cases} \text{find } (\bar{u}_h,\ g_h) \in \mathbb{U}_h(u_0 \circ g_h;\ D) \times T_h(D) \text{ such that} \\ F(\bar{u}_h, g_h;\ D) = \inf_{(\bar{u},g)\in\mathbb{U}_h(u_0\circ g;\ D)\times T_h(D)} F(\bar{u}, g;\ D), \end{cases} \tag{1.3}$$

where D is the computation domain,

$$\mathbb{U}_h(v; D) = \{\bar{u} \in (C(\overline{D}))^m : \bar{u}|_{\partial D_0} = v, \text{and } \bar{u}|_K \text{ is affine } \forall K \in \mathfrak{T}_h(D)\}, \tag{1.4}$$

$$T_h(D) = \{g \in T(D) : g|_K \text{ is affine } \forall K \in \mathfrak{T}_h(D)\}, \tag{1.5}$$

with $\mathfrak{T}_h(D)$ being regular triangulations of D with mesh size h [17] and

$$\begin{aligned} T(D) = \{&\text{bijections } g : \bar{D} \to \bar{\Omega} \,|\, g \in W^{1,\infty}(D;\ \Omega), g^{-1} \in W^{1,\infty}(\Omega;\ D), \\ &g(\partial D_0) = \partial\Omega_0, \text{ and } \det \nabla g > 0, a.e. \text{ in } D\}, \end{aligned} \tag{1.6}$$

and where the functional $F(\cdot,\cdot;\ D)$ is defined by

$$F(\bar{u}, g;\ D) = \int_D f(\nabla \bar{u}(x)(\nabla g(x))^{-1})) \det \nabla g(x)\, dx. \tag{1.7}$$

By setting

$$u(x) = \bar{u}(g^{-1}(x)), \tag{1.8}$$

it is easily seen that

$$F(\bar{u}, g;\ D) = F(u;\ \Omega). \tag{1.9}$$

Compared with the standard finite element method which works on a finite element function space defined on a fixed finite element mesh, the mesh transformation method is actually trying to minimize the energy among finite element functions defined on all admissible finite element mesh distributions. Variant forms and applications of the mesh transformation method can be found in [12, 15, 18, 19, 20, 21, 22], where we see that the application of the mesh transformation method makes it possible for us to obtain numerical results for microstructures with reasonable precision on relatively coarse meshes.

However, the mesh transformation method of the present form has its own problem. Noticing that the set $T_h(D)$ is not closed because of the constraint $\det \nabla g > 0, a.e.$ in D (see (1.6)) and there is no guarantee that a minimizing sequence will not go to the boundary of $T_h(D)$, so we can not prove the existence of solutions for the discrete problem (MTM) (see (1.3)) [12, 18]. In fact, without a control on the quality of the mesh distribution, some of the elements may become increasingly irregular and the determinants of the corresponding mesh mapping gradients $\det(\nabla g)$ tend to zero in the process of energy minimization. Even though a minimizing sequence is enough for our purpose, the poor regularity of the mesh can jeopardize the convergence of the algorithm and prevent us from getting reasonably accurate information on the microstructures. A direct approach for the mesh regularization is to interpolate the numerical solution onto a regular mesh and restart the minimization procedure [19]. However, this usually requires finer and finer mesh, and thus increases the complexity of the computation.

In the present paper, a regularized mesh transformation method is established by adding to the object energy functional $F(\bar{u}, g;\ D)$ in (MTM) (see (1.3)) a mesh quality control term $F_q(\bar{u}, g;\ D)$. A proper choice of $F_q(\bar{u}, g;\ D)$

can guarantee the existence of solutions to the regularized mesh transformation method and can also help to improve the convergence behavior of the corresponding algorithm.

In section 2, a mesh quality control term $F_q(\bar{u}, g;\ D)$, which takes into consideration of conformity (or isotropy) and uniformity (or equi-distribution) [23, 24] of mesh distribution as well as a penalty term on the relative element volume $\det(\nabla g)$ tending to either zero or infinity, is established. In section 3, the regularized mesh transformation method is formulated and analyzed. Numerical examples are given in section 4 to show that the regularized mesh transformation method does help to produce much better numerical results in the computation of microstructures, especially in the simulation of evolution of needle-like microstructures near the austenite-twinned-martensite interface.

2. Conformity, uniformity and quality of mesh distribution

Conformity and uniformity are specially defined measures on the mesh distribution to see how close the mesh is to an ideal one which is of isotropy and equi-distribution in a specially defined geometry, which are usually associated in a certain way to the discrete solution.

Let w be a given function of $x \in \Omega$. One of the simplest ways of defining isotropy and equi-distribution for w in the moving mesh method is to ask the mesh to satisfy the requirements on the graph $\{(x, w(x)) : x \in \Omega\}$, that is the mesh mapping should be chosen such that [24]

$$ds^2 = dx^T dx + (dw)^2 = d\bar{x}^T G^T [I + \nabla w \nabla w^T] G\, d\bar{x} \equiv c\, d\bar{x}^T d\bar{x}, \tag{2.1}$$

where $G = \nabla g(\bar{x})$ is the Jacobian matrix of the mesh mapping g and I is the identity matrix. Let $\lambda_1, \ldots, \lambda_n$ be the eigenvalues of the matrix $B \equiv G^T[I + \nabla w \nabla w^T]G$, then (2.1) leads to (see [24])

$$\lambda_1 = \lambda_2 = \ldots = \lambda_n, \quad \text{Isotropy Criterion;} \tag{2.2}$$

$$(\prod_{i=1}^{n} \lambda_i)^{1/n} = \text{constant}, \quad \text{Equi-distribution Criterion.} \tag{2.3}$$

By the well known arithmetic-mean geometric-mean inequality, we have

$$\frac{1}{n}\sum_{i=1}^{n} \lambda_i \geq (\prod_{i=1}^{n} \lambda_i)^{1/n}, \tag{2.4}$$

where equality holds if and only if (2.2) is satisfied. Since $\sum_{i=1}^n \lambda_i = \mathrm{tr}(B)$ and $\prod_{i=1}^n \lambda_i = \det(B)$, a measure on the conformity may be defined by

$$F_{q,c} \equiv \int_\Omega (\frac{1}{n}\,\mathrm{tr}(B) - (\det(B))^{1/n})\, dx$$
$$= \int_D (\frac{1}{n}\,\mathrm{tr}(B) - (\det(B))^{1/n}) \det(\nabla g)\, d\bar{x}. \quad (2.5)$$

On the other hand, since

$$|\Omega|^{1/2} (\int_\Omega (\det(B))^{2/n}\, dx)^{1/2} \geq \int_\Omega (\det(B))^{1/n}\, dx, \quad (2.6)$$

and the equality holds if and only if $\det(B) =$ constant, or equivalently (2.3) is satisfied, a measure on the uniformity may be defined by

$$F_{q,u} \equiv |\Omega|^{1/2} (\int_\Omega (\det(B))^{2/n}\, dx)^{1/2} - \int_\Omega (\det(B))^{1/n}\, dx$$
$$= |\Omega|^{1/2} (\int_D (\det(B))^{2/n} \det(\nabla g)\, d\bar{x})^{1/2} - \int_D (\det(B))^{1/n} \det(\nabla g)\, d\bar{x} \quad (2.7)$$

In applications, the matrix $[I + \nabla w \nabla w^T]$ is generally replaced by a so called monitor matrix M, which should be chosen according to proper physical and geometrical requirements, and can be also related in some way to the numerical approximation and error estimates [23, 24].

In the present paper, a monitor matrix M of the following form is used,

$$M = \alpha_0 I + \hat{T}^T \hat{T} \quad (2.8)$$

where $\alpha_0 > 0$ is a parameter, and

$$\hat{T} = \det(\nabla u)\ T\ (\nabla u)^{-T} \quad (2.9)$$

is the second Piola-Kirchhoff stress tensor defined on the reference configuration Ω, and where in (2.9) u is the deformation vector and T is the stress tensor which is in general a function of ∇u [25]. The idea of defining the monitor matrix M by (2.8) is that we require that, as for the isotropy criterion, the mesh element is compressed (or stretched) in the direction ν if $|\nu \cdot \hat{T}\nu|$ is large (or small), and as for the equi-distribution criterion, the mesh is denser (or sparser) where $\det \hat{T}$ is larger (or smaller). Since the stress tensor T can be divergent, $\alpha_0 I$ is used to normalize the matrix.

Even though the uniformity quality term $F_{q,u}$ has a control on the uniform distribution of $\det(\nabla g)$, it can not guarantee that $\det(\nabla g)$ is bounded away from zero. In fact, some numerical experiments show that it may allow $\det(\nabla g)$ go to zero on a small amount of elements to achieve more uniformity elsewhere. To ensure that $\det(\nabla g)$ is bounded away from zero, we introduce a relative element volume control term

$$F_{q,r}(g) = \int_D |\log(\det \nabla g)|^\rho \, d\bar{x}, \tag{2.10}$$

where $\rho \in (1, \ \infty)$ is a given constant. Obviously, larger ρ implies tougher penalty on $\det(\nabla g)$ going to either zero or infinity. In our numerical experiments in section 4, $\rho = 2$ is taken.

The quality of the mesh distribution can now be measured by

$$\begin{aligned} & F_q(\bar{u}, g; \alpha_0, \alpha_1, \alpha_2) \equiv \alpha_1 F_{q,c}(\bar{u}, g) + (1-\alpha_1) F_{q,u}(\bar{u}, g) + \alpha_2 F_{q,r}(g) \\ = \ & \alpha_2 \int_D |\log(\det G)|^\rho \, d\bar{x} + \frac{\alpha_1}{n} \int_D \mathrm{tr}(G^T[\alpha_0 \ I + \hat{T}^T \hat{T}]G) \det G \, d\bar{x} \\ & +(1-\alpha_1)|\Omega|^{1/2} \Big(\int_D (\det(\alpha_0 I + \hat{T}^T \hat{T}))^{2/n} (\det G)^{(n+4)/n} \, d\bar{x} \Big)^{1/2} \\ & - \int_D (\det(\alpha_0 I + \hat{T}^T \hat{T}))^{1/n} (\det G)^{(n+1)/n} \, d\bar{x}, \end{aligned} \tag{2.11}$$

where $\alpha_1 \in [0, \ 1]$ is a parameter to control the contributions of conformity and uniformity to the quality of the mesh distribution, and $\alpha_2 > 0$ is a parameter to control the contribution of the relative element volume to the quality of the mesh distribution.

3. Regularized mesh transformation method

As mentioned in the introduction, to avoid the deformed mesh to become highly irregular in the process of solving the discrete problem (1.3), the mesh quality must be brought under control. The simplest way to achieve the goal is to solve (1.3) under a further constraint

$$F_q(\bar{u}, g; \alpha_0, \alpha_1, \alpha_2) \le C, \tag{3.1}$$

for some properly given constant C. However, the control of this constraint on the mesh quality will not take in effect until $F_q(\bar{u}, g; \alpha_0, \alpha_1, \alpha_2) = C$ is reached, and on this level set the control can be very stiff. Another approach is to use the moving mesh method, which improves the mesh quality by decreasing $F_q(\bar{u}, g; \alpha_0, \alpha_1, \alpha_2)$ on the constraint

$$u_{new}(g_{new}(\bar{x}_N)) = u(g_{new}(\bar{x}_N)), \text{ for all nodal points } \bar{x}_N \text{ of } \mathfrak{T}_h(D). \tag{3.2}$$

Because of the highly oscillatory nature of the numerical solutions of our problem, (3.2) can not guarantee that ∇u_{new} is close to ∇u. This implies that an improvement of the mesh quality by the moving mesh method can lead to a significant increase in the elastic energy and thus the algorithm can fail to converge.

In the following, we introduce a new approach. Let

$$\alpha = (\alpha_0, \alpha_1, \alpha_2, \alpha_3) \in A = \{\alpha_0 > 0, \alpha_1 \in [0,\ 1], \alpha_2 > 0 \text{ and } \alpha_3 > 0\}, \tag{3.3}$$

define

$$F_\alpha(\bar{u}, g; D) = F(\bar{u}, g; D) + \alpha_3 F_q(\bar{u}, g; \alpha_0, \alpha_1, \alpha_2). \tag{3.4}$$

The regularized mesh transformation method is defined by replacing the object functional $F(\bar{u}, g; D)$ by $F_\alpha(\bar{u}, g; D)$ in the mesh transformation method. This leads to the following discrete problem (compare with (1.3)):

$$(RMT) \quad \begin{cases} \text{find } (\bar{u}_h,\ g_h) \in \mathbb{U}_h(u_0 \circ g_h;\ D) \times T_h(D) \text{ such that} \\ F_\alpha(\bar{u}_h, g_h;\ D) = \inf_{(\bar{u},g)\in\mathbb{U}_h(u_0\circ g;\ D)\times T_h(D)} F_\alpha(\bar{u}, g;\ D). \end{cases} \tag{3.5}$$

Obviously, larger α_3 implies stronger requirement on the mesh quality, and the mesh transformation method corresponds to $\alpha_3 = 0$.

We have the following existence theorem for the regularized mesh transformation method (3.5):

Theorem 3.1. *Let $\mathfrak{T}_h(D)$ be a regular triangulation of D. Suppose the elastic energy density $f(\cdot)$ is continuously differentiable and satisfies the inequality*

$$C_1 + C_2\|\nabla u\|_p^p \le \int_\Omega f(\nabla u)\, dx \tag{3.6}$$

for all $u \in \mathbb{U}(u_0;\ \Omega)$ and for some constants $C_1 \in R^1$, $C_2 > 0$ and $p > 1$. Then, the discrete problem of the regularized mesh transformation method (3.5) *has at least one solution for any given parameter $\alpha = (\alpha_0, \alpha_1, \alpha_2, \alpha_3) \in A$.*

Proof. Noticing that for a given regular triangulation $\mathfrak{T}_h(D)$ the element volumes are bounded both from below and above by a positive number, thus by the property of the relative element volume control term $F_{q,r}$, we conclude that $\det \nabla g_h$ and $(\det \nabla g_h)^{-1}$ are bounded for a minimizing sequence.

On the other hand, by the inequality (3.6), a minimizing sequence of F_α in $\mathbb{U}_h(u_0 \circ g_h;\ D) \times T_h(D)$ is bounded. Thus, the conclusion of the theorem follows from the standard compactness argument and the continuity of F_α which is a consequence of $f(\cdot)$ being continuously differentiable. □

Theorem 3.2. *Let $\mathfrak{T}_h(D)$ be a regular triangulation of D. Suppose the elastic energy density $f(\cdot)$ is continuously differentiable. Then, for fixed $\alpha_0 > 0$, $\alpha_1 \in [0,\ 1]$ and $\alpha_2 > 0$, we have*

$$\lim_{\alpha_3 \to 0^+} \inf_{(\bar{u},g)\in \mathbb{U}_h(u_0\circ g;\ D)\times T_h(D)} F_\alpha(\bar{u}, g;\ D) = \inf_{(\bar{u},g)\in \mathbb{U}_h(u_0\circ g;\ D)\times T_h(D)} F(\bar{u}, g;\ D). \tag{3.7}$$

Proof. For given $\varepsilon > 0$, let $(\bar{u}_h, g_h) \in \mathbb{U}_h(u_0 \circ g_h;\ D) \times T_h(D)$ be such that

$$F(\bar{u}_h, g_h;\ D) < \inf_{(\bar{u},g)\in \mathbb{U}_h(u_0\circ g;\ D)\times T_h(D)} F(\bar{u}, g;\ D) + \varepsilon. \tag{3.8}$$

By the assumption that $f(\cdot)$ is continuously differentiable, we conclude that $F_q(\bar{u}_h, g_h;\ \alpha_0, \alpha_1, \alpha_2)$ is finite. Thus , we have

$$\lim_{\alpha_3 \to 0^+} \inf_{(\bar{u},g)\in \mathbb{U}_h(u_0\circ g;\ D)\times T_h(D)} F_\alpha(\bar{u}, g;\ D) < \inf_{(\bar{u},g)\in \mathbb{U}_h(u_0\circ g;\ D)\times T_h(D)} F(\bar{u}, g;\ D) + \varepsilon. \tag{3.9}$$

Since $\varepsilon > 0$ is arbitrary and F_q is non-negative, the inequality (3.9) implies the equation (3.7). □

Theorem 3.2 together with the approximation property of the mesh transformation method [12, 18] show the convergence of the regularized mesh transformation method.

Remark 3.1. The reason that the continuously differentiable condition on $f(\cdot)$ is assumed in the above existence and convergence theorems of the regularized mesh transformation method is that the stress tensor T, which involves the differentials of $f(\cdot)$, is used in the monitor function M. In general, the condition is not necessary and can be replaced by some weaker conditions.

4. Numerical examples

In our numerical examples, we consider a two dimensional ($n = m = 2$) Ericksen-James type elastic energy density of the form [4, 25]

$$f(\nabla u,\ \theta) = \Phi(C,\ \theta), \tag{4.1}$$

and

$$\Phi(C,\ \theta) = \frac{b(\theta)}{4}(C_{11}-C_{22})^2 - \frac{c(\theta)}{8}(C_{11}-C_{22})^2|C_{11}-C_{22}| + \frac{d(\theta)}{16}(C_{11}-C_{22})^4 + e_1 C_{12}^2 + e_2(\operatorname{tr} C - 2)^2, \quad (4.2)$$

where $C = (\nabla u)^T \nabla u \in \mathbb{S}^n = \{A \in \mathbb{R}^{n\times n} : A^T = A\}$, which is the set of symmetric matrices in R^n, is the right Cauchy-Green strain tensor,

$$b(\theta) = (1 + \alpha \arctan \mu(\theta - \theta_T)) d_0 \hat{\varepsilon}^2, \quad (4.3)$$

$$c(\theta) = 2(1 + \frac{1+2\gamma}{3}\alpha \arctan \mu(\theta - \theta_T)) d_0 \hat{\varepsilon}, \quad (4.4)$$

$$d(\theta) = (1 + \gamma\alpha \arctan \mu(\theta - \theta_T)) d_0, \quad (4.5)$$

and where $d_0 > 0$, $e_1 > 0$ and $e_2 > 0$ are the elastic moduli, $\hat{\varepsilon}$ is the transformation strain, θ_T is the transformation temperature,

$$\alpha \approx \frac{2}{\pi}, \ \ \mu > 0, \ \text{and } \gamma < 1 \quad (4.6)$$

are the material constants used to reflect the change of elastic moduli and the energy barriers as the temperature varies.

The energy density $f(\nabla u,\ \theta)$ defined by (4.1)-(4.6) has the following properties [19, 21, 22]:

(i): a unique potential well $SO(2)$ for $\theta > \theta_T$;
(ii): two potential wells $SO(2)U_0$ and $SO(2)U_1$ for $\theta < \theta_T$,

where $SO(2)$ is the set of all 2×2 rotational matrices, and

$$U_0 = \begin{pmatrix} \sqrt{1-\hat{\varepsilon}} & 0 \\ 0 & \sqrt{1+\hat{\varepsilon}} \end{pmatrix}, \quad U_1 = \begin{pmatrix} \sqrt{1+\hat{\varepsilon}} & 0 \\ 0 & \sqrt{1-\hat{\varepsilon}} \end{pmatrix}. \quad (4.7)$$

Furthermore, U_0 and $R^{\pm}U_1$ are in rank-one connection. More precisely, let $\eta_1 = \sqrt{1-\hat{\varepsilon}}$ and $\eta_2 = \sqrt{1+\hat{\varepsilon}}$ and let

$$R^{\pm} = \begin{pmatrix} \eta_1\eta_2 & \pm\hat{\varepsilon} \\ \mp\hat{\varepsilon} & \eta_1\eta_2 \end{pmatrix}, \quad (4.8)$$

then, we have

$$R^{\pm}U_1 = U_0 + \mathbf{a}^{\pm} \otimes \mathbf{n}^{\pm}, \quad (4.9)$$

where $\mathbf{a}^{\pm} = \sqrt{2}\hat{\varepsilon}(\eta_1,\ \mp\eta_2)^T$ and $\mathbf{n}^{\pm} = \frac{1}{\sqrt{2}}(1,\ \pm 1)^T$.

In our numerical experiments, we set the elastic constants $\alpha = 2.02/\pi$, $\mu = 0.25$, $\gamma = 0$, $\hat{\varepsilon} = 0.05$, $d_0 = 500$, $e_1 = 3.5$ and $e_2 = 15$. The transformation temperature is taken to be $\theta_T = 70\,^{\circ}$C.

Example 1. Let the temperature $\theta \equiv 60\,^{\circ}$C, which is below the transformation temperature. Let $u_0(x) = A^+_\lambda x$ with $A^+_\lambda = (1-\lambda)U_0 + \lambda R^+ U_1$, and let $\partial\Omega_0 = \partial\Omega$. Then the minimizing sequence of $F(u;\,\Omega)$ in $\mathbb{U}(u_0;\ \Omega)$ (see (1.1) and (1.2)) leads to a simple laminated microstructure composed of two variants of martensite U_0 and R^+U_1 with corresponding volume fractions $(1-\lambda)$ and λ for any open set Ω [1, 2].

We apply the regularized periodic relaxation method, that is the regularized mesh transformation method combined with the periodic relaxation method [18], to compute the laminated microstructure. Let the computation domain $D = (-1,\ 1)^2$, and let $\mathfrak{T}_h(D)$ be a family of regular triangulations of D, where $h = h_N = 2\sqrt{2}/N$ with $N \geq 2$, introduced by the lines

$$\begin{cases} x = -1 + \frac{2}{N}i, & 0 \leq i \leq N; \\ y = -1 + \frac{2}{N}j, & 0 \leq j \leq N; \\ y = \pm(x + 2 - \frac{4}{N}k), & 0 < k < N. \end{cases}$$

Let

$$S_i^{\pm}(D) = \{x = (x_1, x_2) \in \partial D : x_i = \pm 1\}, \quad i = 1, 2$$

and let

$$V(D) = \{x = (x_1, x_2) \in \partial D : x_1, x_2 = \pm 1\}.$$

For a given rotational matrix $R \in SO(2)$, define

$$\begin{aligned} P(D;R) = \{&g \in (W^{1,\infty}(D))^2 : g^{-1} \in (W^{1,\infty}(g(D)))^2 \text{ and } \det \nabla g > 0, \\ &a.e. \text{ in } D,\ g(x) = R\,x, \forall x \in V(D), (g-R)|_{S_i^+} = (g-R)|_{S_i^-}, i = 1, 2\}. \end{aligned}$$

Obviously, the image $g(D)$ of a map $g \in P(D;R)$ is a periodic domain with its four vertices coinciding with those of $R(D)$. The admissible mesh mapping sets $T(D)$, $T_h(D)$ (see (1.6) and (1.5)) are relaxed respectively to

$$P(D) = \{g \in P(D;R) : \text{for some } R \in SO(2)\}, \tag{4.10}$$

$$P_h(D) = \{g \in P(D) : g|_K \text{ is affine } \forall K \in \mathfrak{T}_h\}. \tag{4.11}$$

To relax the deformation boundary condition, we rewrite the deformation in the form of $A_\lambda^+ x + u(x)$, and thus u has zero boundary condition and $F(u;\Omega)$ and $F(\bar{u}, g; D)$, where $\bar{u}(\bar{x}) = u(g(\bar{x}))$, can be rewritten as

$$F(u;\Omega) = \int_\Omega f(A_\lambda^+ + \nabla u(x), \theta(x))\, dx$$

and

$$F(\bar{u}, g; D) = \int_D f(A_\lambda^+ + \nabla \bar{u}(x)(\nabla g(x))^{-1}), \theta(x)) \det \nabla g(x)\, dx.$$

The admissible deformation sets are periodically relaxed to

$$\tilde{\mathbb{U}}(0; D) = \{\bar{u} \in W^{1,\infty}(D;\ \mathbb{R}^2) : \bar{u}(x) = 0, \forall x \in V(D), \qquad \bar{u}|_{S_i^+(D)} = \bar{u}|_{S_i^-(D)}, i = 1, 2\}, \tag{4.12}$$

$$\tilde{\mathbb{U}}_h(0; D) = \mathbb{U}_h \cap \tilde{\mathbb{U}}(0; D). \tag{4.13}$$

Thus, the discrete problem of the regularized periodic relaxation method (RPR) is formulated as (compare with (3.5)):

$$(RPR) \qquad \begin{cases} \text{find } (\bar{u},\ g) \in \tilde{\mathbb{U}}_h(0;\ D) \times P_h(D) \text{ such that} \\ F_\alpha(\bar{u}, g;\ D) = \inf_{(\bar{u}', g') \in \tilde{\mathbb{U}}_h(0;\ D) \times P_h(D)} F_\alpha(\bar{u}', g';\ D). \end{cases} \tag{4.14}$$

With similar arguments as in section 3 and using the convergence result of the periodic relaxation method [18], it is not difficult to show that the results in section 3 can be extended to the regularized periodic relaxation method.

In our numerical experiments, a 4×4 mesh ($N = 4$), which is sufficient for a simple laminated microstructure [18], is used and the conjugate gradient method is applied in searching for the minimizers of the discrete problem (RPR). We start with an initial mesh mapping $g_0(\bar{x}) = R(\tau)\bar{x}$ and an initial deformation $\bar{u}_0$ given by a random data with uniform distribution on $[-0.05,\ 0.05]$. Take $\lambda = 0.2$ and $(\alpha_0, \alpha_1, \alpha_2) = (1.0, 0.85, 1.0)$. If we start with $\tau = 0.0$ and $\alpha_3 = 10^{-8}$, then the conjugate gradient method produces numerical results with highly irregularly deformed elements as shown in Figure 1. In fact, without sufficient mesh quality control (in particular when there is no mesh quality control, that is when $\alpha_3 = 0$), the conjugate gradient search starting with a sufficiently small τ generally leads to such numerical results. On the other hand, If we start with $\tau = 0.0$ and $\alpha_3 = 10^{-4}$, and reduce α_3 to

10^{-8} after some convergent criterion, say $\|\partial F_\alpha/\partial(\bar{u}, g)\| < 10^{-6}$(TOL), is satisfied, then a much sharp numerical result with higher mesh quality as shown in Figure 2 is obtained. In Table 1, the numerical results with initial $\alpha_3 = 10^{-8}$ and 10^{-4} and final $\alpha_3 = 10^{-8}$ with final tolerance TOL$= 10^{-7}$ are compared, where $E_r(energy)$ is the relative error of the elastic energy of the laminated microstructure, $E_r(\lambda)$ is the relative error of the volume fraction λ. It is clearly seen that the mesh quality control does help a great deal in this case to produce much sharper numerical results on the laminated microstructure.

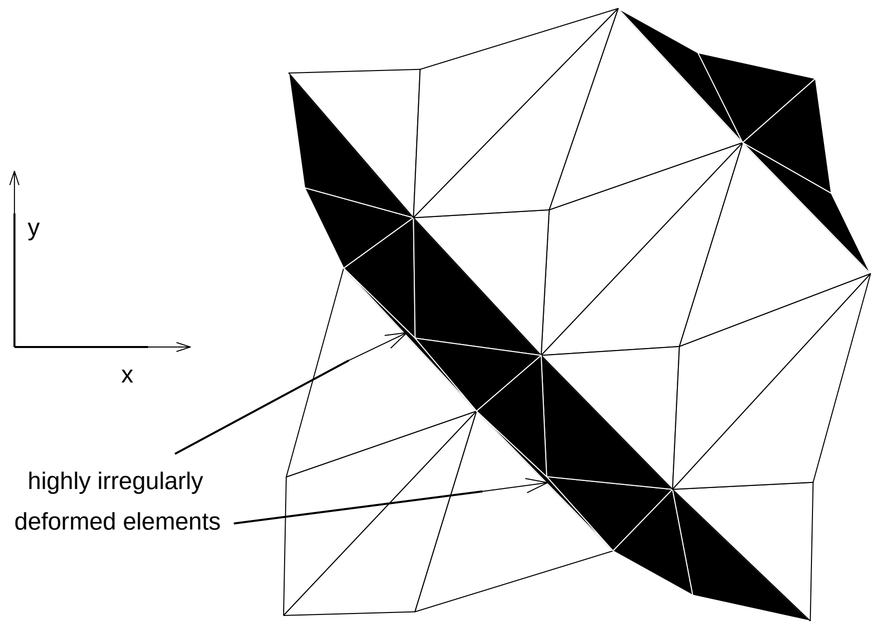

FIGURE 1. Periodic microstructure block with irregularly deformed mesh obtained by CG search starting with $\alpha_3 = 10^{-8}$.

TABLE 1. Comparison of numerical results.

initial α_3	final α_3	$E_r(energy)$	$E_r(\lambda)$	mesh quality F_q
10^{-8}	10^{-8}	6.272×10^{-2}	1.679×10^{-1}	4.54
10^{-4}	10^{-8}	7.696×10^{-9}	6.050×10^{-5}	2.79

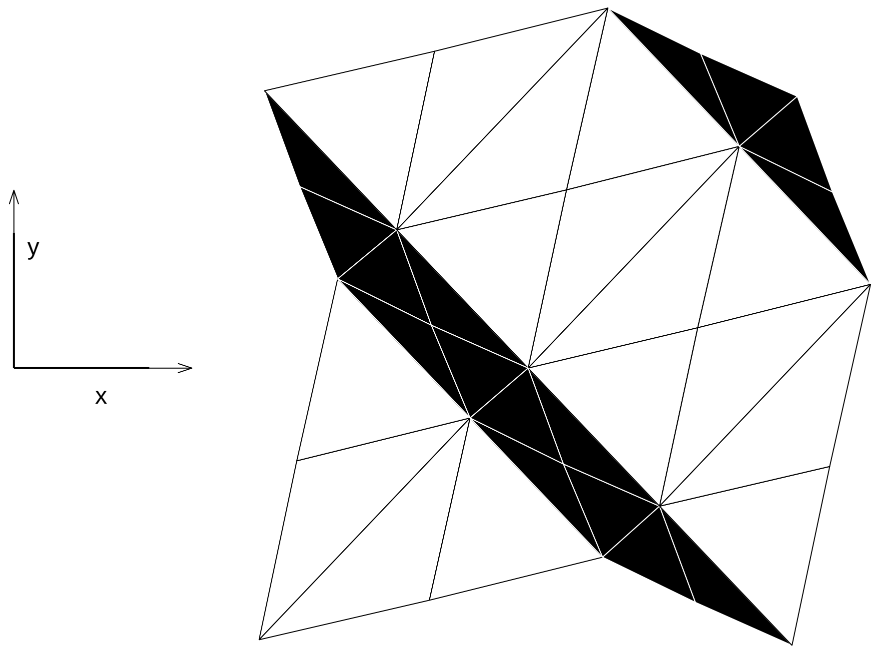

FIGURE 2. Periodic microstructure block with regularly deformed mesh obtained by CG search staring with $\alpha_3 = 10^{-4}$.

Example 2. Let $\hat{D} = (-5,\ 5) \times (-1,\ 1)$, let $D = \Omega = R(\tau)\hat{D}$ with $\tau = \pi/4$, where $R(\tau) \in SO(2)$ is a rotational matrix with rotation angle τ. Let

$$\partial\Omega_{\pm} = R(\tau)\{(\hat{x}_1, \hat{x}_2)^T : \hat{x}_1 = \pm 5, |\hat{x}_2| \leq 1\},$$

and let the boundary condition be given by $u_0(x) = x$ for $x \in \partial\Omega_0 = \partial\Omega_-$. Let

$$\theta(x; \theta_-, \theta_+) = \theta_- + 0.1 \times (\theta_+ - \theta_-)(5 + x_1 \cos\tau + x_2 \sin\tau) \tag{4.15}$$

be a temperature distribution given on $\bar{\Omega}$, which assumes given temperatures θ_- on $\partial\Omega_-$ and θ_+ on $\partial\Omega_+$ respectively and is linearly distributed in between. If $\theta_- > \theta_T$ and $\theta_+ < \theta_T$, where θ_T is the transformation temperature, and if a twin laminates with the interfaces normal to $\mathbf{n}^- = \frac{1}{\sqrt{2}}(1,\ -1)^T$, for example a twin laminates composed of U_0 and $R^- U_1$, is formed in a neighborhood of $\partial\Omega_+$, then the twin laminates will develop into needle like microstructures with the needle tips pointing toward the $\partial\Omega_-$ direction. The needles will grow toward the $\partial\Omega_-$ direction as the temperature rises, and recede accordingly as the temperature falls.

Since the needle tips are very sharp, the elements near the needle tips are generally highly irregularly deformed. This causes serious problems for the simulation of the growth of the needles as the temperature distribution changes. One way to overcome the difficulty is to interpolate the numerical solution on a regular mesh and restart the minimizing procedure [19]. In the following we take a more general new approach, that is to apply the regularized mesh transformation method to compute the growth of the needle-like laminated microstructure, which is easier to implement and works well on much coarser meshes.

Let $\mathfrak{T}_h(\hat{D})$ be a family of regular triangulations of $\hat{D}$ introduced by the lines

$$\begin{cases} \hat{x} = -5(1 + \frac{2}{M} i), & 0 \le i \le M; \\ \hat{y} = -1 + \frac{2}{N} j, & 0 \le j \le N; \\ \hat{y} = \pm(1 + \frac{M}{5N}(\hat{x} + 5) - \frac{4}{N} k), & 0 < k < \frac{M+N}{2}. \end{cases}$$

Let $\mathfrak{T}_h(D) = R(\tau)\mathfrak{T}_h(\hat{D}) \equiv \{R(\tau)K : \forall K \in \mathfrak{T}_h(\hat{D})\}$. In our numerical experiments, we take $M = 10$ and $N = 12$, and take mesh quality control parameters $(\alpha_0, \alpha_1, \alpha_2) = (1.0,\ 0.85,\ 1.0)$.

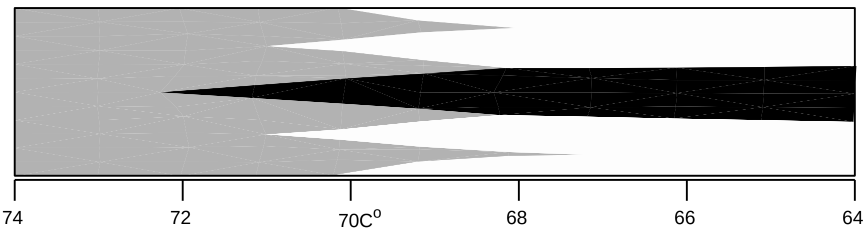

FIGURE 3. Original needle-like laminates for $\theta_- = 74^\circ$C and $\theta_+ = 64^\circ$C.

For $\theta_- = 74^\circ$C and $\theta_+ = 64^\circ$C, a needle-like laminated microstructure as shown in Figure 3, where an element is painted white, black or grey according to whether the deformation gradient is closer to $SO(2)U_0$, $SO(2)U_1$ or $SO(2)$ respectively, is given on Ω, which may be obtained by applying a proper

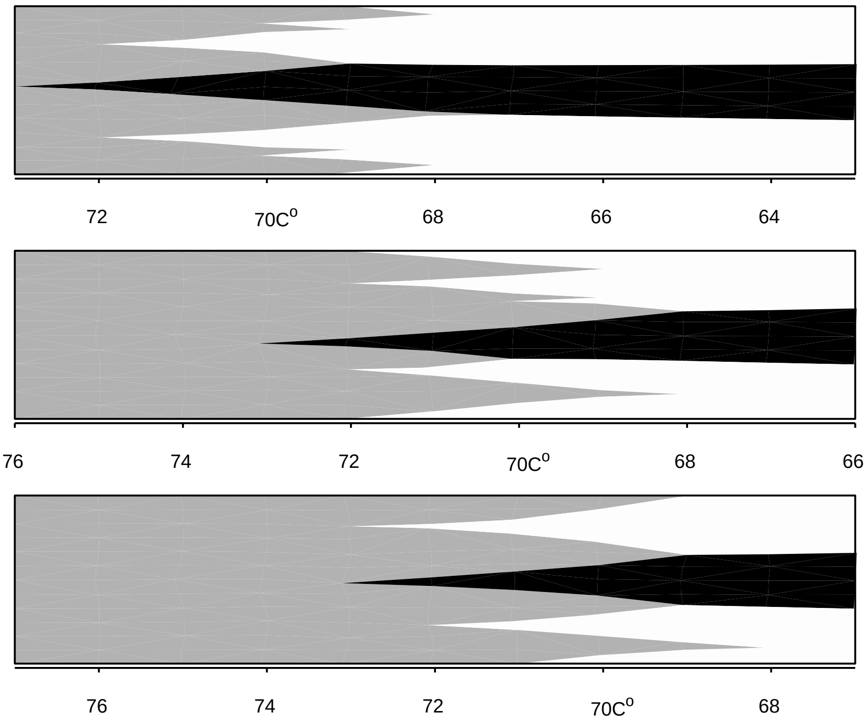

FIGURE 4. Needle-like laminates evolved from the original one for various temperature distributions.

bending load on $\partial\Omega_+$ and by applying the mesh transformation method [26]. Taking this needle-like laminate as the initial data, and applying the conjugate gradient method to solve the discrete problem introduced by the regularized mesh transformation method (RMT) (see (3.5)), where the mesh quality control parameter $\alpha_3 = 10^{-3}$ is taken initially and reduced gradually to 10^{-8} in the process of minimization, we obtain the numerical results as shown in Figure 4 for temperature distributions given by (4.15) with $\theta_- = 73\,^\circ$C and $76\,^\circ$C, $\theta_+ = 63\,^\circ$C and $66\,^\circ$C respectively. Taking the numerical result for $\theta_- = 76\,^\circ$C, $\theta_+ = 66\,^\circ$C as the initial data and in the same way, we obtain the numerical result for the case where $\theta_- = 77\,^\circ$C and $\theta_+ = 67\,^\circ$C, which is also shown in Figure 4. As a comparison, the numerical results obtained with essentially no mesh quality control (with $\alpha_3 \equiv 10^{-8}$) are shown in Figure 5.

We point out here that for sharp numerical results of the needle-like laminates a highly irregular mesh is inevitable, since the needle tips are very sharp, however the regularized mesh transformation method prevents the irregularity from happening elsewhere. We notice also that, in the simulation of needle

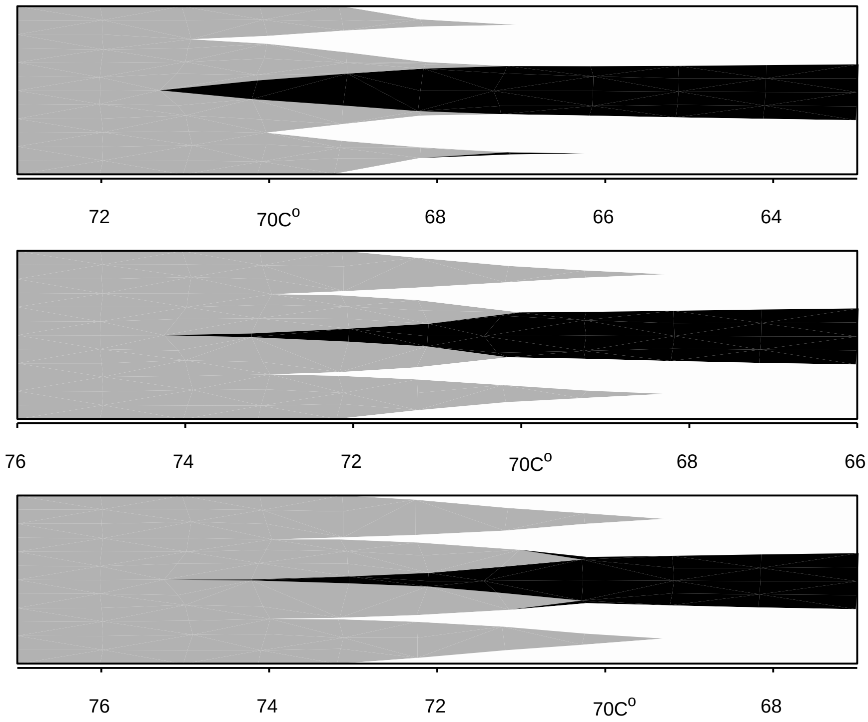

FIGURE 5. Needle-like laminates evolved from the original one for various temperature distributions with essentially no mesh quality control.

growth, the larger penalty, which corresponds to larger α_3, initially imposed on the mesh irregularity reduces the mesh irregularity near the needle tips, so that the phase transition is computed on a more regularized mesh by the mesh transformation method, furthermore the irregular mesh element will be regularized when they are no longer a part of a needle tip.

Remark 4.1. Our numerical examples clearly show that the mesh quality control term does have a significant role in the regularized mesh transformation method. However, we must bear in mind that it is the elastic energy that we want to minimize, the mesh quality control term is in fact mainly used to help us to find a better search direction. Hence the role of the mesh quality here in the regularized mesh transformation method is very different from that in the moving mesh method, where the mesh quality is suppose to reflect the approximation property of a mesh for a given function through a properly defined monitor function [23, 24].

References

[1] J. M. Ball and R. D. James, *Fine phase mixtures as minimizers of energy.* **Arch. Rat. Mech. Anal., 100**(1987)1, 13-52.

[2] J. M. Ball and R. D. James, *Proposed experimental test of a theory of fine microstructure and the two-well problem.* **Phil. Trans. R. Soc. London 338A**(1992), 389-450.

[3] C. Collins and M Luskin, *The computation of the austenitic-martensitic phase transition.* In **Partial Differential Equations and Continuum Models of Phase Transitions** Lecture Nodes in Physics, Vol. 344, M. Rascle, D. Serre and M. Slemrod, eds, Springer-Verlag, New York, (1989), pp. 34-50.

[4] P. Klouček and M. Luskin, *The computation of the dynamics of the martensitic transformation*, **Continuum Mech. Thermodyn., 6**(1994), 209-240.

[5] M. Luskin, *On the computation of crystalline microstructure.* **Acta Numerica, 5**(1996), 191-257.

[6] R. A. Nicolaides, N. Walkington and H. Wang, *Numerical methods for a nonconvex optimization problem modeling martensitic microstructure*, SIAM J. SCI. Comput, 18(1997), 1122-1141.

[7] G. Dolzmann, *Numerical computation of rank-one convex envelopes.* **SIAM J. Numer. Anal., 36**(1999), 1621-1635.

[8] G. Dolzmann and N. J. Walkington, *Estimates for numerical approximations of rank-one convex envelopes.* **Numer. Math., 85** (2000), 647-663.

[9] M. K. Gobbert and A. Prohl, *A discontinuous finite element method for solving a multiwell problem.* **SIAM J Numer. Anal. 37**(1999), 246-268.

[10] M.K. Gobbert and A. Prohl, *A comparison of classical and new finite element methods for the computation of laminated microstructure*, **Appl. Numer. Math. 36**(2001), 155-178.

[11] Z.-P. Li, *Finite order rank-one convex envelopes and computation of microstructures with laminates in laminates.* **BIT Numer. Math., 40**(4)(2000), 745-761.

[12] Z.-P. Li, *A mesh transformation method for computing microstructures.* **Numer. Math., 89**(2001), 511-533.

[13] C. Collins, *Computation of twinning*, in **Microstructure and Phase Transitions**, IMA Volumes in Mathematics and Its Applications, Vol.54, J. Ericksen, R. James, D. Kinderlehrer and M. Luskin, eds, Springer-Verlag, New York, (1993), 39-50.

[14] C. Collins, M. Luskin and J. Riordan, *Computational results for a two-dimensional model of crystalline microstructure*, in **Microstructure and Phase Transitions**, IMA Volumes in Mathematics and Its Applications, Vol.54, J. Ericksen, R. James, D. Kinderlehrer and M. Luskin, eds, Springer-Verlag, New York, (1993), 51-56.

[15] Z.-P. Li, *Rotational transformation method and some numerical techniques for the computation of microstructures.* **Math. Models Meth. Appl. Sci., 8**(1998), 985-1002.

[16] Z.-P. Li, *Laminated microstructure in a variational problem with a non-rank-one connected double well potential*, **J. Math. Anal. Appl., 217**(1998), 490-500.

[17] P.G. Ciarlet, **The Finite Element Method for Elliptic Problems**. North-Holland, Amsterdam, 1978.

[18] Z.-P. Li, *A periodic relaxation method for computing microstructures*. **Appl. Numer. Math., 32**(2000), 291-303.

[19] Z.-P. Li, *Mesh transformation and regularization in numerical simulation of austenitic-martensitic phase transition*. **Comp. Material Sci., 21**(2001), 418-428.

[20] Z.-P. Li, *Computations of needle-like microstructures*, **Appl. Numer. Math., 39**(2001), 1-15.

[21] Z.-P. Li, *A numerical study on the scale of laminated microstructure with surface energy*. **Materials Sci. Eng., A 343**(2003), 182-193.

[22] Z.-P. Li, *Numerical justification of branched laminated microstructure with surface energy*. **SIAM J. Sci. Computing, 24**(3)(2003), 1054-1075.

[23] W. Huang, *Practical aspect of formulation and solution of moving mesh partial differential equations*. **J. Comput. Physics, 171**(2001), 753-775.

[24] W. Huang, *Variational mesh adaption: isotropy and equidistribution*. **J. Comput. Physics, 174**(2001), 903-924.

[25] P. G. Ciarlet, **Mathematical Elasticity**, Volume 1: Three Dimensional Elasticity. North-Holland, Amsterdam, 1988.

[26] Z.-P. Li, *Numerical computation of stress induced microstructure*. **Science in China, A 47**, supp. (2004), 165-171.

E-mail address: `lizp@math.pku.edu.cn`